LAWRENCE
LIVERMORE
NATIONAL
LABORATORY

LLNL-JRNL-611032

# Upgraded Analytical Model of the Cylinder Test

P. C. Souers, L. Lauderbach, R. Garza, L. Ferranti, P. Vitello

January 17, 2013

Propellants, Explosives, Pyrotechnics

## Disclaimer

# Upgraded Analytical Model of the Cylinder Test

**P. Clark Souers*[a], Lisa Lauderbach, Raul Garza, Louis Ferranti, Jr. and Peter Vitello**

**Abstract:** A Gurney-type equation was previously corrected for wall thinning and angle of tilt, and now we have added shock wave attenuation in the copper wall and air gap energy loss. Extensive calculations were undertaken to calibrate the two new energy loss mechanisms across all explosives. The corrected Gurney equation is recommended for cylinder use over the original 1943 form. The effect of these corrections is to add more energy to the adiabat values from a relative volume of 2 to 7, with low energy explosives having the largest correction. The data was pushed up to a relative volume of about 15 and the JWL parameter $\omega$ was obtained directly. The total detonation energy density was locked to the v = 7 adiabat energy density, so that the Cylinder test gives all necessary values needed to make a JWL.

Keywords: Cylinder test, detonation energy, Gurney equation, Cyclex, JWL

## 1 Introduction

The Cylinder test is a calibrated pipe-bomb used as the only means of obtaining detonation energy densities while the detonation is proceeding [1-4]. The output is annealed copper wall velocity as a function of time. The square of the velocity is proportional to the detonation energy density, $E_d$, at a specific relative volume, v. A common practice is to use the 1943 Gurney equation to calculate the energy density [5]. In our terminology, at a given relative volume, v, this is [6]

$$E_d = \left\{ \frac{\rho_m}{2} \left( \frac{(S_o + X_o)^2 - S_o^2}{S_o^2} \right) + \frac{\rho_o}{4} \right\} u_o^2 \qquad (1)$$

where $\rho_m$ and $\rho_o$ are the initial copper and explosive densities, $S_o$ is the scaled inner radius (always 12.7 mm), $X_o$ the scaled wall thickness and $u_o$ is the measured wall velocity perpendicular to the axis, as is the case with a streak camera. (Scaled means that distance and time are divided by the number of inches diameter of the explosive. Converting to mythical 12.7 mm-radius [1-inch diameter] cylinders allows comparison of all cylinder data.) Eq. 1 assumes the same wall thickness always, so we created to a wall-thinning version [3]

$$E_d = \left\{ \rho_m \left( \frac{S + X}{S_o} \right)^2 \ln\left( \frac{S + X}{S} \right) + \frac{\rho_o}{4} \left( \frac{S + X}{S} \right)^2 \right\} u_o^2 \,, \qquad (2)$$

where S and X are the inner radius and wall thickness at a later time during expansion.

To make the JWL Equation-of-State, we use special $E_d$ points at scaled outer wall "standard" displacements of 6, 12.5 and 19 mm. The relative volume, v, is obtained from

$$v \approx \left( \frac{S}{S_o} \right)^2 \tag{3}$$

which makes use of the geometry in this highly confined experiment. For the displacements listed above, v is set at 2.4, 4.4 and 7.0, respectively.

All modern cylinders are "full-wall", which means the wall thickness is $1/5^{th}$ the inner radius. Twenty years ago, "half-wall" cylinders, with $1/10^{th}$ the radius, were tried as a means of obtaining higher resolution. The coming of Fabry-Perot interferometry [7] and photonic Doppler velocimetry [8] rendered half-wall tubes obsolete, but their legacy was to show the importance of the tilt angle of the copper $\Theta$ and the angle of the PDV probes, $\alpha$ [4]. A certain amount of confusion has existed in deciding what the new laser methods actually measure. Souers suggested that the copper particle velocity angle is about half of $\Theta$ [9]. Goosman et al. measured the velocity of an angled bullet on the side, at the $45^o$ angle and at the front and concluded that Fabry measured only the velocity in the direction of the probe [10]. The side view gave a zero result, even though the material was moving at full speed through the laser spot. Briggs et al. did the same angled bullet experiment with PDV [11], and a similar result with rotating disks was reported by Dolan [12]. This means that the laser-measured velocity is a Doppler velocity, not a spot velocity as seen by the streak camera.

The easiest derivation of the copper tilt angle is given by Eqs. A-1 and A-2 in the Appendix. From the laser, the angle comes from an arcsin; from the streak camera, it comes from an arctangent. The tilt angle is about $12^o$ for a full-wall tube and it increases slowly with time.

The coming of Fabry-Perot interferometry gave more accurate wall velocities. The Fabry and streak camera data taken on the same samples is shown in Table 1 for full and half-wall tubes. We see a difference, which is larger for half-wall tubes. This led to the development of an angle model, which is fully described for the first time in the Appendix. It may be simplified so that the Fabry/PDV energy equation becomes [4]

$$E_d(laser) \approx \left\{ \rho_m \left( \frac{S+X}{S_o} \right)^2 \ln\left( \frac{S+X}{S} \right) + \frac{\rho_o}{4} \left( \frac{S+X}{S} \right)^2 \right\} \left( \frac{u_\alpha}{\cos\Theta} \right)^2 \quad (4)$$

where $u_a$ is now the measured velocity at the PDV angle of $\alpha$.

Steve Pemberton suggested that low energy explosives might not be self-similar in the Cylinder Test because the sound speed of the shock wave in the copper wall is faster than the detonation velocity [13]. However, earlier modeling showed a precursor shock in the wall ahead of the detonating explosives but the system came to steady state [14]. Four urea nitrate and shotgun powder shots showed self-similar behavior although one Kinepak (AN 79/NM 21) shot out of two did not, possibly because of a defective tube [15].

**Table 1.** Ratios of Fabry /streak camera velocities at the three scaled displacements in copper.

| Shot No. | explosive | diameter mm | wall thickness mm | Fabry/Streak Velocity at Displacements mm 6 | 12.5 | 19 |
|---|---|---|---|---|---|---|
| Full-Wall | | | | | | |
| 573 | **RX-43-AB** | 25.4 | 2.59 | 0.981 | 0.978 | |
| 574 | **RX-43-AC** | 25.4 | 2.59 | 0.979 | 0.984 | |
| 575 | **RX-45-AA** | 25.4 | 2.59 | 0.984 | 0.982 | |
| 580 | **PBXNC-19** | 25.4 | 2.60 | 0.990 | 0.966 | 0.978 |
| Average | | | | 0.984 | 0.978 | 0.978 |
| Half-Wall | | | | | | |
| 549 | **RX-39-AA** | 25.4 | 1.36 | | 0.971 | 0.964 |
| 564 | **RX-39-AB** | 25.4 | 1.36 | 0.972 | 0.971 | 0.966 |
| 547 | **LX-04** | 50.8 | 2.71 | 0.971 | 0.961 | 0.966 |
| 586 | **PETN** | 25.4 | 1.37 | 0.990 | 0.973 | 0.966 |
| 560 | **RX-41-AB** | 25.4 | 1.36 | 0.977 | 0.972 | 0.965 |
| 585 | **RX-52-AE** | 50.8 | 2.72 | 0.976 | 0.970 | 0.967 |
| Average | | | | 0.977 | 0.970 | 0.966 |

## 2 Experimental

In the last two years, we have designed shots with six to eight PDV probes along the cylinder. The probes are set at LLNL at $7^o$ with more robust aluminum frame construction to maintain the

angle. The data appears good out to a relative volume of about 15. Figure 1 shows a picture of an annealed copper cylinder with the center being at about v = 16. The sides are showing “stretch marks”, but not breakthrough, but these marks could scatter the laser beam. Figure 2 shows two measured velocity traces with data-ending glitches at about v = 13 to 15. Even so, we have added new “standard” points at the scaled displacements of 25.5 and 32 mm, representing v = 10 and 13.5 .

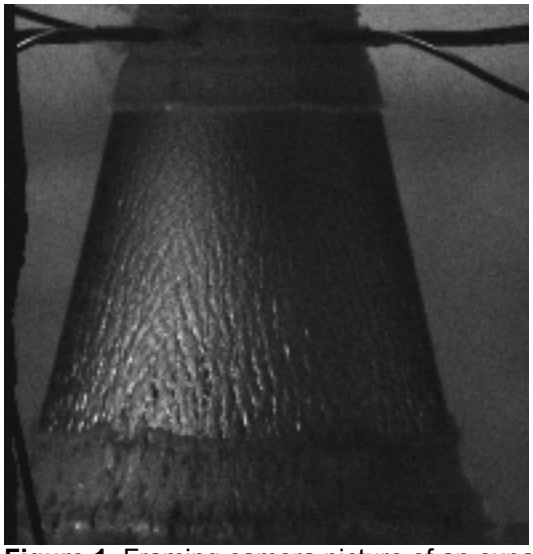

**Figure 1.** Framing camera picture of an expanding unannealed copper tube with stretch marks on the outside beginning at about v = 15.

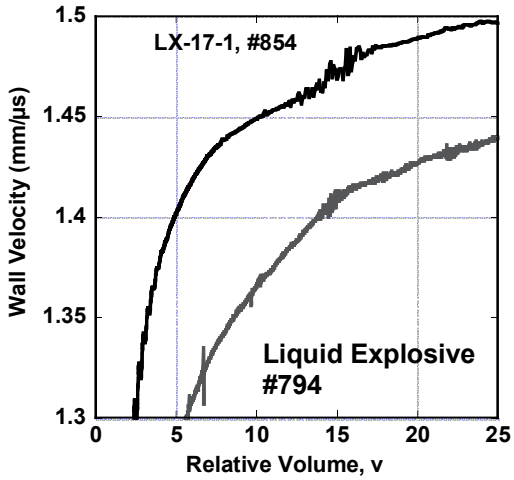


**Figure 2.** Two measured PDV velocity traces with surface glitches beginning at v = 13 to 15.

More pictures should be taken of the expanding cylinder. If the stretch marks always appear, then a copper cylinder cannot be lengthened indefinitely in order to get ever-larger relative volumes. Perhaps another material might be more ductile.

Figure 3 compares data accuracy in fitting for probes in the center of the copper tube with those near the end, where the gas leaves before the final desired expansion is achieved. This shows that the same information is contained by the end probes but its accuracy is less.

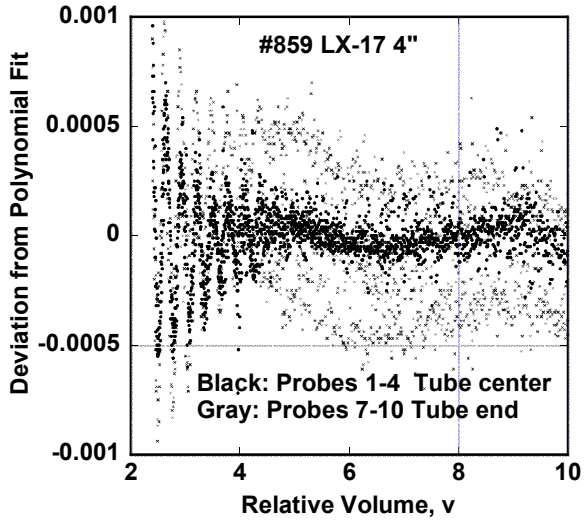


**Figure 3.** Comparison of data accuracy for probes in the center and at the end of the tube.

The Cylinder test delivers the detonation energy density, which in JWL formulation is

$$E_d = E_o - \left[ \frac{A}{R_1} \exp(-R_1 v) + \frac{B}{R_2} \exp(-R_2 v) + \frac{C}{\omega v^{\omega}} \right] \tag{5}$$

For v > 7, the C term alone matters, so that

$$E_d = E_o - \frac{C}{\omega v^{\omega}}, \quad v \geq 7 \ . \tag{6}$$

Then, using a value of $E_o$, we can get $\omega$ from

$$\frac{\omega 7^{\omega}}{\omega 10^{\omega}} = \frac{E_o - E_d(10)}{E_o - E_d(7)} . \tag{7}$$

In order to get $\omega$ in Eq. 7, we need to know $E_o$, the total detonation energy density. We have used CHEETAH to construct this relation for all CHNO explosives. We have

$$E_o(kJ\ cm^3) = 0.7791 + 1.373\left[E_d(7.0)\right] - 0.02356\left[E_d(7.0)\right]^2. \quad (8)$$

This allows all physical variables needed for the JWL to be defined systematically from the Cylinder test.

### 3 Results

Table 2 shows various $\omega$ values derived from Eq. 7. Although the errors could be $\pm$0.06 because of the uncertainty in $E_o$, we still have explosives either high, medium or low in the list.

**Table 2.** Derived values of $\omega$.

| Explosive | $\omega$ measd |
|---|---|
| **PETN**, 0.75-1.765 g/cc | 0.34-0.39 |
| **High % HMX** | 0.33 |
| **High % RDX** | 0.32 |
| **EGDN** | 0.29 |
| **urea nitrate** | 0.24 |
| **Potass. chlorate, perchlorate** | 0.19 |
| **High % TATB** | 0.16-0.17 |

What does $\omega$ mean? We can derive it roughly from these equations

$$P = \frac{\nu z R T}{V} \approx \frac{\nu \omega C_P T}{V}, \quad (9)$$

where P is the pressure, $\nu$ the number of gas moles per mol of initial explosive, z the compressibility, R the molar gas constant, T the temperature, V the molar volume, and $C_P$ is an average heat capacity along the adiabat. The first term on the right is the gas equation and the second is from Ignition & Growth [16]. If we take the last two terms, we have

$$\omega \approx \frac{\langle z \rangle}{\langle C_P \rangle} R \quad (10)$$

where the compressibility and heat capacity are further averaged over v > 7 to the end. Because most explosives are all CHNO, their terms in Eq. 10 do not change much and we do not expect $\omega$ to vary more than a factor of 2 to 3. CHEETAH calculations show that $\omega$ is not a constant and it is likely that we define it so only to match the JWL format.

**4 Code Analysis**

The code is a Lagrange descendant of the finite-element CALE with Eulerian relaxation applied where desired. The wall velocities and expansion were checked using tracer particles corrected for the direction of observation. The actual dimensions of the cylinders were used, which ranged from 12.7 to 101.6 mm-diameters. The air gaps between the inner copper wall and the outside of the explosive were explicitly modeled. We used programmed burn with square zones at 80 zones/cm scaled to 25.4 mm diameter. This means that a 12.7-mm tube was run at 160 zones/cm, 50.8 mm at 40 and 101.6 mm at 20 zones/cm. We created new JWL's with slightly different energy densities until we were within ½% of the measured wall velocities at v = 2.4, 4.4 and 7.0. About two-dozen explosives of all types and densities were checked.

Because our copper is annealed, we changed the Steinberg-Guinan [17,18] half-hard yield stress to 0.049 GPa and the ultimate yield stress to 0.26 GPa, as based on commercial copper data [19, 20].

The final equations, for both streak and laser (PDV and Fabry-Perot), become

$$E_d(\mathit{streak},\ \mathit{gap}) = \left\{ \rho_m \left(\frac{S+X}{S_o}\right)^2 \ln\left(\frac{S+X}{S}\right) + \frac{\rho_o}{4}\left(\frac{S+X}{S}\right)^2 \right\} \left[ \left(\frac{R_o}{R_{\exp}}\right) u_o (1+\lambda X_o) \right]^2 \qquad (11)$$

$$E_d(\mathit{laser\ gap}) = \left\{ \rho_m \left(\frac{S+X}{S_o}\right)^2 \ln\left(\frac{S+X}{S}\right) + \frac{\rho_o}{4}\left(\frac{S+X}{S}\right)^2 \right\} \left[ \left(\frac{R_o}{R_{\exp}}\right) \left(\frac{u_\alpha}{\cos\Theta}\right) (1+\lambda X_o) \right]^2 \qquad (12)$$

Two new corrections are present. The shock wave attenuation in the copper wall is described by the $X_o$ term, where $X_o$ is the scaled initial wall thickness. The coefficient of $\lambda$ = 0.009 $mm^{-1}$ is found empirically by fitting the liquid and powder samples which have no air gap effect. The ratio of initial radii describe the air gap energy loss, where $R_{exp}$ is the initial unscaled explosive radius

and $R_o$ is the initial unscaled inner radius of the copper tube. $(R_o/R_{exp})^2$ represents the extra volume with energy added if the gap did not exist.

Our attenuation coefficient agrees well with Los Alamos Dural aluminum plate experiments, where the free-surface velocity was measured as a function of the plate thickness [21]. An average of $\lambda = 0.01$ mm$^{-1}$ was found.

A comparison of all the corrections is shown in Table 3 for a dense and powdered explosive. First, we list the Gurney energy from Eq. 1, then the adjustment for wall thinning and edge angle from Eq. 4. The final corrections from Eq. 12 are last. The effect is to raise the energy density with each correction, with the %-differences being larger for the smaller energies.

**Table 3.** Comparison of Gurney detonation energy densities at v = 2.4 for a pressed and powdered explosive.

| | $E_d(2.4)$ | kJ cm$^{-3}$ |
|---|---|---|
| | PBX 9407 | Kinepak |
| | 1.63 g cm$^{-3}$ | 1.20 g cm$^{-3}$ |
| Gurney equation | 5.33 | 2.03 |
| Wall Thinning, angle | 5.50 | 2.09 |
| Correct for Hydrocode | 5.71 | 2.18 |

**5 Uncertainties**

An obvious uncertainty is the definition of the relative volume, which actually is a function of the wall thickness and the tilt angle. For a 6 mm wall displacement, we find a full-wall v of 2.38 and a half-wall of 2.28. We don't want the analytical model to become too complicated, so the standard relative volumes 2.4, 4.4 and 7.0 are easy-to-remember constant values, which really work best for modern full-wall tubes.

We get our standard velocities by integrating the velocity to get wall displacement, and then plotting velocity vs. displacement. For simplicity, we assume that the same displacements apply to streak and laser. However, the difference between streak and laser is roughly cos$\beta$, where $\beta$ is about 7$^o$, which creates a 1% error at the most.

These errors are now absorbed by the attenuation and air gap corrections.

**6 Conclusions**

The considerably corrected Gurney equation gives a more accurate description of the energy density of the Cylinder test and should be used in place of the original. Copper appears useful up to relative volumes of 15. Self-similar behavior has generally been found at all explosive energies.

**Appendix. Rigid Wall Angle Model**

This model assumes that the copper wall folds outward like a door on hinges. The schematic defining the angles is shown in Figure A1. At the bottom is the outer copper wall, now bent at time t at an angle $\Theta$ to the cylinder axis. The vector $u_m$ is perpendicular to the wall with the angle $\Theta$. It is referenced to the perpendicular to the initial wall. The vector $u_\beta$ is the actual metal particle velocity at the angle $\beta$. The PDV probe looks in at the angle $\alpha$, which we set at $7^o$, so that it is close to $\beta$. The probe vector $u_\alpha$ is the Doppler velocity as seen at the angle $\alpha$, □□. the projection of $u_\alpha$ on $u_\beta$. Streak camera data is only taken at $0^o$ along the vector $u_o$. This vector is not a Doppler velocity but is phase or laser-spot move-velocity determined by differentiating distance and time. A look at $0^o$ shows new metal moving past. Finally, the vectors xdot and ydot are components of $u_\beta$, and they are given by our computer model, so that $\beta$ can be determined by calculating. From Figure A1, we see these relations.

$$\sin\Theta = \frac{u_m}{U_s} \tag{A-1}$$

$$tan\Theta = \frac{u_o}{U_s} \tag{A-2}$$

$$\cos(\beta - \alpha) = \frac{u_\alpha}{u_\beta} \tag{A-3}$$

$$tan\beta = \frac{xdot}{ydot} \tag{A-4}$$

$$\cos(\Theta - \beta) = \frac{u_m}{u_\beta} \tag{A-5}$$

$$\cos\Theta = \frac{u_m}{u_o} \tag{A-6}$$

$$\sin\beta = \frac{xdot}{u_\beta} \tag{A-7}$$

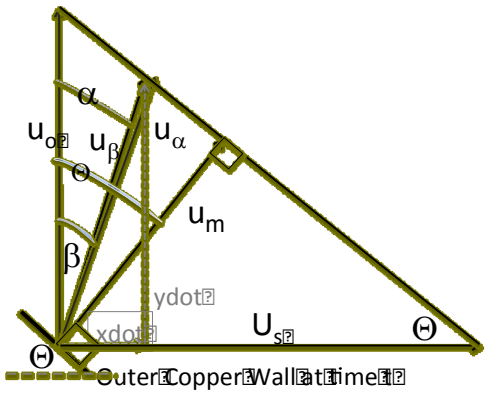


Figure A1. Schematic of the titled copper cylinder wall at time t with the various velocity vectors and angles. All the activity is outside the copper wall. The angles $\alpha$ and $\beta$ are about the same.

Angle $\Theta$ is an important variable of the measurement. For the streak camera, we get it from Eq. A-2. For the PDV and Fabry, we use Eqs. A-1, A-3 and A-5 to get

$$\frac{u_\alpha}{U_s} = \frac{\cos(\beta-\alpha)\sin\Theta}{\cos(\Theta-\beta)} \approx \sin\Theta, \tag{A-8}$$

That $\beta \approx \Theta/2$ has been confirmed using the code. From above, we take Eqs. A-3, A-5 and A-6, which we combine into

$$\frac{u_\alpha}{u_o} = \frac{\cos(\beta-\alpha)\cos\Theta}{\cos(\Theta-\beta)} \approx \cos\Theta. \tag{A-9}$$

A typical full-wall angle is $12^o$, which gives 0.984, which agrees with the measured Fabry/streak camera ratios in Table 1. The ratio is larger for half-wall tubes because $\Theta$ is larger.

**Acknowledgments**

This work performed under the auspices of the U. S. Department of Energy by Lawrence Livermore National Laboratory under Contract DE-AC52-07NA27344.

*Symbols*

| | |
|---|---|
| A | JWL high-pressure parameter/ GPa |
| $\alpha$ | Fabry or PDV probe angle/ degrees |
| B | JWL intermediate-pressure parameter/ GPa |
| $\beta$ | metal wall particle velocity angle/ degrees |
| C | JWL low-pressure Parameter/ GPa |
| $C_P$ | heat capacity at constant pressure/ J $mol^{-1}K^{-1}$ |
| $<C_P>$ | average heat capacity at constant pressure/ J $mol^{-1}K^{-1}$ |
| $E_d$ | detonation energy density at some relative volume/ kJ $cm^{-3}$ |
| $E_o$ | total detonation energy density/ kJ $cm^{-3}$ |
| $g_o$ | partially scaled initial air gap between explosive and copper/ mm |
| $\lambda$ | copper shock wave attenuation coefficient/ $\mu s^{-1}$ |
| P | pressure/ GPa |
| R | gas constant/J $mol^{-1}$ $K^{-1}$ |
| $R_{exp}$ | initial unscaled radius of explosive/ mm |
| $R_o$ | initial unscaled inner radius of metal cylinder cylinder/ mm |
| $R_1$ | JWL high-pressure exponent |
| $R_2$ | JWL intermediate-pressure exponent |
| $\rho_m$ | initial metal wall density/ g $cm^{-3}$ |
| $\rho_o$ | initial explosive density/ g $cm^{-3}$ |
| S | scaled outer cylinder radius at later time/ mm |
| $S_o$ | scaled initial outer cylinder radius/ mm |
| T | temperature/ K |
| t | time/ $\mu s$ |
| $\Theta$ | metal wall tilt angle/ degrees |
| $U_s$ | detonation velocity/ mm $\mu s^{-1}$ |
| $u_\alpha$ | metal wall velocity at probe angle/ mm $\mu s^{-1}$ |
| $u_\beta$ | metal wall velocity at particle velocity angle/ mm $\mu s^{-1}$ |
| $u_m$ | metal wall velocity perpendicular to wall/ mm $\mu s^{-1}$ |
| $u_o$ | metal wall velocity perpendicular to axis/ mm $\mu s^{-1}$ |
| V | molar volume/ $cm^3$ $mol^{-1}$ |
| v | relative volume |
| X | scaled wall thickness at later time/ mm |
| $X_o$ | initial scaled wall thickness/ mm |
| xdot | axial particle velocity in the code/ mm $\mu s^{-1}$ |
| $x_o$ | partially scaled initial wall thickness/ mm |
| ydot | radial particle velocity in the code/ mm $\mu s^{-1}$ |
| $\omega$ | JWL low-pressure exponent |
| z | compressibility of gas products |
| <z> | average compressibility of gas products |

**References**


[1] J. W. Kury, H. C. Hornig, E. L. Lee, L. McDonnel, D. L. Ornellas, M. Finger, F. M. Strange and M. L. Wilkens, "Metal Acceleration by Chemical Explosives," *Proceedings of the Fourth Symposium (International) on Detonation*, White Oak, MD, October 12-15, **1965**, pp. 3-12.

[2] P. C. Souers and J. W. Kury, "Comparison of Cylinder Data and Code Calculations for Homogeneous Explosives," *Propellants, Explosives, Pyrotechnics* **1993***, 18*, 175-183.

[3] John E. Reaugh and P. Clark Souers, "A Constant-Density Gurney Approach to the Cylinder Test," *Propellants, Explosives, Pyrotechnics* ***2004****, 29*, 124-128.

[4] P. C. Souers, Raul Garza, Howard Hornig, Lisa Lauderbach, Cinda Owens and Peter Vitello, "Metal Angle Correction in the Cylinder Test," *Propellants, Explosives, Pyrotechnics* **2011***, 36* [1], 9-15.

[5] L. G. Hill, "Detonation Product Equation-of-State directly from the Cylinder test," *21st International Symposium on Shock Waves*, Great Keppel Island, Queensland, Australia, July 20-25, **1997**; also LANL report LA-UR-97-2213, CONF-970764-3,**1997**.

[6] R. W. Gurney, *The Initial Velocities of Fragments from Bombs, Shells and Grenades*, Army Ballistic Research Laboratory, report BRL 405,**1943**.

[7] C. F. McMillan, D. R. Goosman and and N. L. Parker "Velocimetry of Fast Surfaces Using Fabry-Perot Interferometry," *Rev. Sci. Instrum.* **1988***, 59*, [1], 1-21.

[8] O. T. Strand, D. R. Goosman, C. Martinez, T. L. Whitworth and W. W. Kuhlow, "A Novel System for High-Speed Velocimetry using Heterodyne Techniques," *Revs. Sci. Intrs.* **2006***, 77*, 083108.

[9] P. C. Souers and L. C. Haselman, Jr., *Detonation Equation of State at LLNL. 1993*, Lawrence Livermore National Laboratory UCRL-ID-116113, March, **1964**, pp. 4-2, 4-3, 4-8.

[10] D. R. Goosman, A. M. Frank, H. H. Chau and N. L. Parker, "Fabry-Perot Velocimetry Techniques: Is Doppler Shift affected by Surface Normal Direction?", *Proceedings of the Society of Photo-Optical Instrumentation Engineers* **1983***, 427*, pp. 127-135.

[11] M. E. Briggs, L. M. Hull and M. A. Shinas, "Fundamental Experiments in Velocimetry," *Shock Compression of Condensed Matter – 2009*, M. J. Elert, et. al., eds., American Institute of Physics **2009**, *1195*, pp. 577-580.

[12] D. H. Dolan, "What does "Velocity" Interferometry really Mean," *Shock Compression of Condensed Matter – 2009*, M. J. Elert, et. al., eds., American Institute of Physics, **2009**, *1195*, pp. 589-593.

[13] S. Pemberton, Los Alamos National Laboratory, private communications, **2010-2012**.

[14] P. C. Souers, P. Vitello, S. Esen and H. A. Bilgin, "The Effects of Containment on Detonation Velocity," *Propellants, Explosives, Pyrotechnics* **2004***, 29* [1], 19-26.

[15] P. C. Souers, L. Lauderbach, K. Moua and R. Garza, "Size Effect and Cylinder Test on Several Commercial Explosives," *7th Biennial Conference of the American-Physical-Society-Topical-Group on Shock Compression of Condensed Matter*, AIP Conference Proceedings, **2010**, *1426,* pp. 343-346.

[16] E. L. Lee and C. M. Tarver, “Phenomological Model of Shock Initiation in Heterogeneous Explosives,” *Phys. Fluids* **1980**, 23 [12], 2362-2372.

[17] D. J. Steinberg, S. G. Cochran and M. W. Guinan, “A Constitutive Model for Metals applicable at High Strain-Rate,” *J. Appl. Phys.* **1980***, 51* [3], 1498-1504.

[18] D. J. Steinberg, *Equation of State and Strength Properties of Selected Materials*, Lawrence Livermore National Laboratory, Livermore, CA 94551, report UCRL-MA-106439, **1991**.

[19] E. Jordan Brooks Corp., Phoenix, AZ, http://ejbmetals.com/pdf/datasheets-metal_strip/Ca101-102.pdf, **2012**.

[20] DIYTrade Corp., Ningbo, China, http://www.diytrade.com/china/pd/6103193/OFHC_COPPER.html, **2012**.

[21] LASL Explosive Property Data, T. R. Gibbs and A, Popolato, eds., University Of California Press, Berkeley, **1980**, pp. 261-279.

*[a] Energetic Materials Center, Lawrence Livermore National Laboratory, Livermore, CA USA 94550, souers1@llnl.gov.